Supporting Information

The facile fabrication and high-performance sensing for glucose of sea-urchin-like CoFeLDH/PBA/NF heterojunction

Tian Liu, Chen Chen, Dengke Xiong, Jiang Wang, Chunxiao Lu, Shuanglu Ying, Yuxuan Kong, Fei-Yan Yi*

School of Material Science and Chemical Engineering, Ningbo University, Ningbo, Zhejiang, 315211, P. R. China

1. Experimental Section

1.1 Materials.

Cobalt nitrate hexahydrate ($Co(NO_3)_2 \cdot 6H_2O$), Anhydrous dextrose, Aodium citrate ($C_6H_5Na_3O_7 \cdot 2H_2O$) and Sodium chloride (NaCl) were purchased from Sinopharma chemical reagent Co., Ltd. Potassium ferricyanide ($K_3[Fe(CN)_6]$) and Dopamine hydrochloride (DA) were supplied by Shanghai Macklin Biochemical Co., Ltd. Ascorbic acid (AA) and Uric acid (UA) were acquired from Shanghai yuanye Bio-Technology Co., Ltd. Urea ($CO(NH_2)$) was acquired from Aladdin, and Iron nitrate nonahydrate ($Fe(NO_3)_3 \cdot 9H_2O$) was acquired from Rhawn. All chemicals in the experiment were used without further treatment.

1.2.1 Preparation of CoFePBA/NF.

Ni foams was prepared according to a previous literature.[1] All Ni foams (NF, 30×30 mm) were ultrasonicated in 3 M hydrochloric acid (HCl), DI water and ethanol for 15 min successively to remove the surface oxide layer. Then they were dried in an air oven overnight at 60 °C. In a typical procedure, $Co(NO_3)_2 \cdot 6H_2O$ (0.1746 g) and $C_6H_5Na_3O_7 \cdot 2H_2O$ (0.2647 g) were dissolved in 20 mL DI water to form a uniform solution A. $K_3[Fe(CN)_6]$ (0.1317 g) were dissolved in 20 mL DI water to obtain a transparent solution B. Solution A was quickly poured in solution B under stirring and stirred for 10 min. Then a piece of pre-treated NF was immersed in the above mixed solution at room temperature without any interruption for 18 h. Then, the NF covered with CoFePBA was taken out, washed with DI water and ethanol repeatedly and dried in air oven at 60 °C for 12 h to obtained CoFePBA/NF.

1.2.2 Preparation of CoFeLDH/PBA/NF.

The as-prepared CoFePBA/NF was placed into 50 mL Teflon lined stainless steel autoclave with $Co(NO_3)_2 \cdot 6H_2O$ (0.1455 g), $Fe(NO_3)_3 \cdot 9H_2O$ (0.404 g) and $CO(NH_2)$ (0.3602 g) and 35 mL DI water. The

mixture was maintained at 120 °C for 7 h and then cooled to room temperature naturally. The target composite was taken out and washed with DI water and ethanol several times and then dried in an oven overnight at 60 °C to obtained CoFeLDH/PBA/NF.

1.3 Characterization.

Scanning electron microscopy (SEM) images were acquired from field-emission scanning electron microscope (FEI Nova Nano SEM 450). Atomic force microscope (AFM) patterns were tested on a Bruker-Icon. Transmission electron microscopy (TEM), HRTEM and SAED images were acquired from transmission electron microscope (FEI Tecnai G2 F20). X-ray powder diffraction (XRD) patterns were recorded on an X-ray powder diffractometer (Bruker D8 Advance, using Cu Ka radiation). Fourier transform infrared (FT-IR) spectra was obtained by using a Fourier transform infrared spectrometer (FT-IR, Bruker INVENIO S). X-ray photoelectron spectroscopy (XPS) analysis was conducted by a spectrometer (Thermo Scientific K-Alpha), using Al Ka radiation exciting source.

1.4 Electrochemical measurements

The electrochemical tests were carried out at room temperature in a CHI 760E electrochemical workstation (Chenhua, Shanghai, China) using 0.1 M NaOH (100 mL) aqueous electrolyte. The as-prepared CoFeLDH/PBA/NF sample (10×10 mm^2), platinum sheet and Ag/AgCl electrode (in saturated KCl solution) were served as working electrode, counter electrode and reference electrode, respectively. As a comparison, the glucose detection performance of bare NF and CoFePBA/NF was tested. Cyclic voltammetry (CV) measurements were used to investigate the electrocatalytic activity towards glucose, the reaction kinetics of CoFeLDH/PBA/NF electrode as well as the selection of electrolyte pH. Most of the CV tests are carried out in the potential range of -0.2-0.8V, except for ECSA in the non-Faraday region (-0.1-0 V). Chronoamperometry measurements were carried out at potential of 0.5 V under uniform stirring conditions to evaluate the sensitivity, selectivity, anti-interference property and reproducibility of CoFeLDH/PBA/NF nanocomposite. Amperometric response of five CoFeLDH/PBA/NF electrodes fabricated at the same condition was recorded respectively towards the addition of 30 μM glucose at potential of 0.5 V to assess reproducibility. The limit of detection (LOD) of the sensor is estimated using the equation, as follows.[2]

$$LOD = \frac{3s_b}{slope}$$

where s_b is the standard deviation obtained from 10 measurements of the blank signal, and slope is the slope value of the calibration plot.
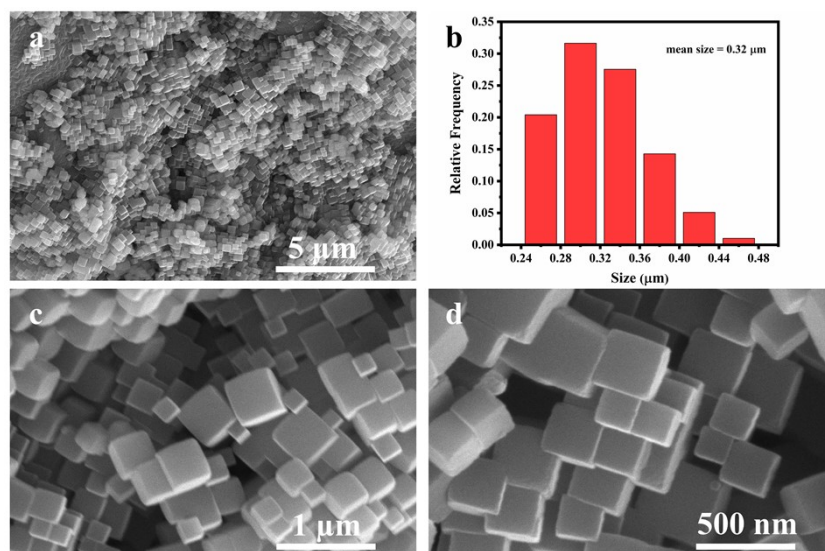

Fig. S1 (a, c-d) SEM images of CoFePBA/NF. (b) Size distribution histogram of CoFePBA nanocubes according to the SEM image of Fig. S1a.
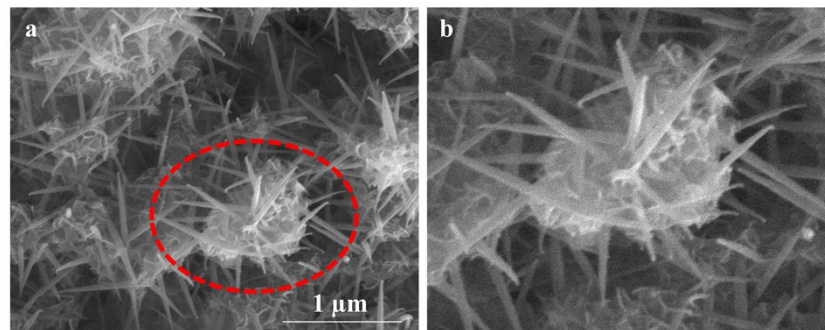

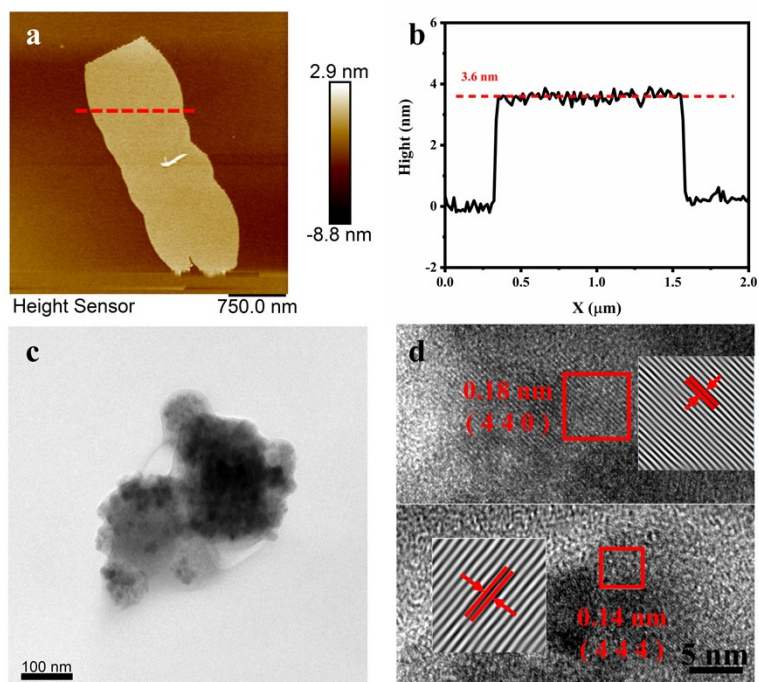**Fig. S2** (a) SEM images of CoFeLDH/PBA/NF. (b) Enlargement of Fig. S2a.

Fig. S3 AFM images of flaky area of the CoFeLDH/PBA/NF (a) and corresponding height curves (b). TEM (c) and HRTEM (d) image of the flaky area of CoFeLDH/PBA/NF.
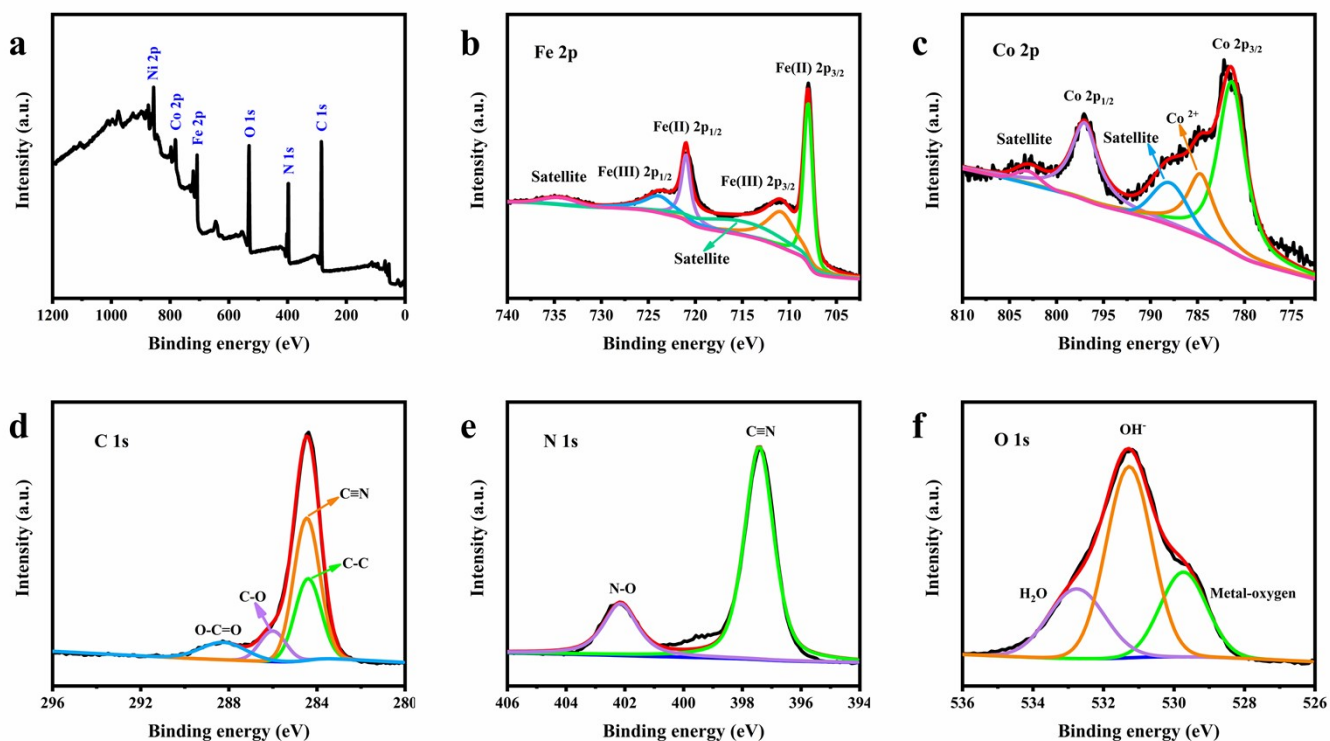

Fig. S4 (a) XPS spectrum of CoFeLDH/PBA/NF. High-resolution XPS spectra of Fe 2p (b), Co 2p (c), C 1s (d), N 1s (e) and O 1s (f) for CoFeLDH/PBA/NF.

To further analyze the elemental compositions and chemical state in target CoFeLDH/PBA/NF composite, X-ray photoelectron spectroscopy (XPS) was monitored. As depicted in Fig. S4a, the full XPS spectrum of

sample indicates the co-exist of Fe, Co, C, N and O elements. In Fe 2p spectrum as shown in Fig. S4b, the peaks located at 723.9 eV and 710.9 eV with two satellite peaks of 734.4 eV and 715.1 eV can be attributed to Fe(III) $2p_{1/2}$ and Fe(III) $2p_{3/2}$, respectively.[3, 4] The Fe $2p_{1/2}$ and Fe $2p_{3/2}$ peaks locate at 721.0 eV and 708.0 eV, respectively, which are characteristic of Fe(II) from CoFePBA.[5] For Co 2p spectrum (Fig. S4c), two main peaks at 797.0 eV and 781.4 eV are assigned to Co(II)$2p_{1/2}$ and Co(II) $2p_{3/2}$, respectively, together with two satellite peaks at 803.0 eV and 787.9 eV. The peak at binding energy of 784.7 eV is also assigned to Co(II).[4] For the C 1s spectrum (Fig. S4d), the peaks located at 288.3 eV, 286 eV, 284.5 eV and 284.4 eV were assigned to the characteristic of O-C=O, C-O, C≡N and C-C, respectively. For the spectrum of N 1s in Fig. S4e, the peaks located at 402.1 eV and 397.4 eV can be assigned to N-O and C≡N, respectively.[5] For the O 1s spectrum (Fig. S4f), the binding energy at 532.8 eV and 529.7 eV corresponds to the H_2O and metal oxygen bonding. The peak situated at 531.3 eV is ascribed to OH^- group from the CoFeLDH.[6]
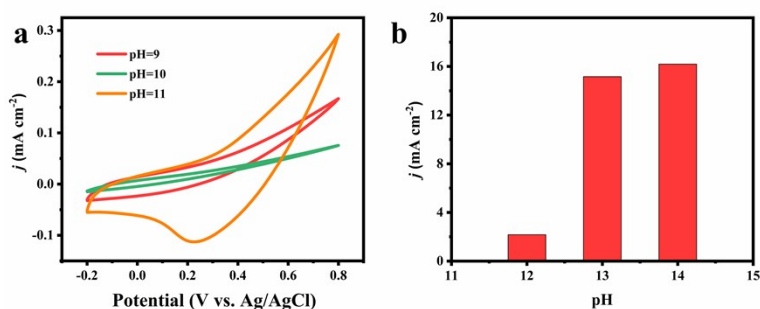

Fig. S5 (a) CV curves of CoFeLDH/PBA/NF in different pH with 30 μM glucose at 50 mV s^{-1}. (b) The plot of oxidation peak current density and pH.

The pH of supporting electrolyte has a great influence on the electrochemical signal.[7-8] Electrochemical detection of glucose in acid-supported electrolytes has not been reported due to the low glucose activity under acidic conditions. A few non-enzyme glucose sensors chose neutral PBS solution as the supporting electrolyte.[9-11] For non-enzyme glucose sensors, alkaline NaOH solution with a concentration of 0.1 M is usually selected as supporting electrolyte.[10,11] In order to estimate the influence of pH in the alkaline range on electrochemical response, CoFeLDH/PBA/NF electrode was investigated under electrolyte with different pH values of 9-14. As shown in Fig. S5a, when the pH is 9 or 10, there is no obvious redox peak, and when the pH is 11, there is only an oxidation peak, indicating that it is not suitable for detection in such an environment. Then, the pH value of NaOH solution continues to increase from 12 to 14, the relationship between oxidation peak current density and pH values (12-14) is shown in Fig. S5b, showing that the oxidation peak current also increases with the increase of pH value. When pH is 13 or 14, the peak current

shows clear enhancement. 1 M NaOH solution of pH=14 was usually used as electrolyte in oxygen evolution reaction.[12,13] Thus, when pH is 14, such electrocatalytic oxygen evolution reaction will interfere the oxidation of glucose. Hence, the electrolyte of 0.1 M NaOH of pH =13 is selected for electrochemical sensing tests.
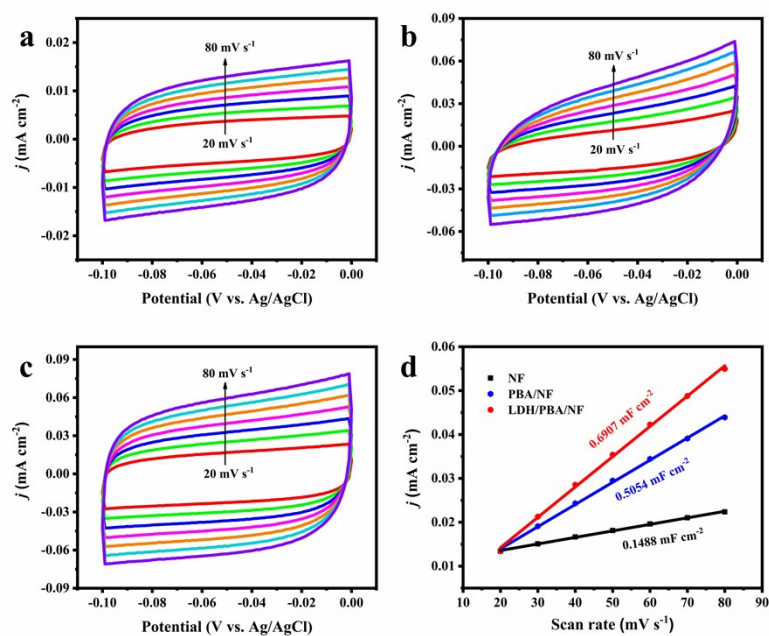

Fig. S6 CV curves at scan rate of 20-80 mV s^{-1} of NF (a), CoFePBA/NF (b), and CoFeLDH/PBA/NF (c). (d) The plot of $\Delta j/2$ ($\Delta j = j_a - j_c$) against scan rates.

In order to further estimate the electrocatalytic activity for target CoFeLDH/PBA/NF, and precursors of CoFePBA/NF and NF, their electrochemically active surface area (ECSA) data was obtained. It is well known that ECSA result is proportional to double-layer capacitances (C_{dl}), so C_{dl} value can directly reflect the level of ECSA. C_{dl} value was obtained based on cyclic voltammograms (CV) curves in the range of a non-Faradaic potential region with different scan rates. Herein, these CV curves are measured in the non-Faraday potential range of -0.1-0 V (vs Ag/AgCl) in 0.1 M NaOH, as shown in Fig. S6a-c. Fig. S6d shows that target CoFeLDH/PBA/NF electrode achieved the highest C_{dl} value than CoFePBA/NF and NF. Larger ECSA result stands for more active sites and surface area. ECSA results provide more deep insight to explain the improved electrocatalytic activity towards glucose for as-prepared CoFeLDH/PBA/NF, further demonstrating the importance and necessity of such design in this work.
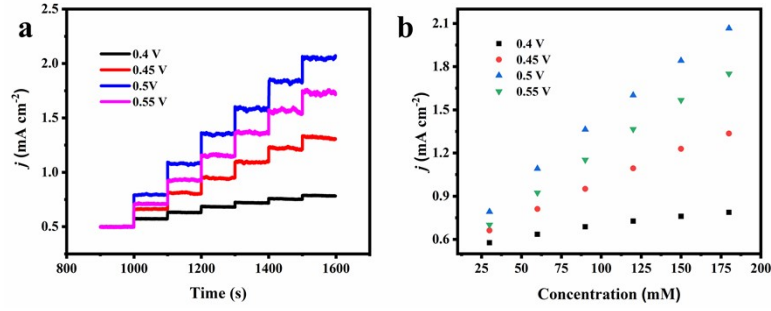
Fig. S7 (a) Amperometric responses of CoFeLDH/PBA/NF electrode at potentials of 0.40-0.55 V with continuous addition of 30 μM glucose in 0.1 M NaOH. (b) The changes of peak current density among glucose concentration.

Table S1. Comparison of the performance of glucose sensor based on CoFeLDH/PBA/NF electrodes with previous reported related LDH or PBA composites electrodes.

| Electrode materials	Sensitivity ($\mu A\ mM^{-1}\ cm^{-2}$)	Linear range (μM)	Detection limit (μM)	References
NiCo PBA hollow nanocubes	149	2-3790	1.2	12
NiFe PBA	2392.07	0.5-2165.5	0.8621	15
CoFe LDH/Ni wire	1063	10-1000	0.27	16
CoFe-LDH/manganese porphyrin	25.6	100-10000	1.4	17
CuO/CoNi-LDHs	~~	0.1-384	0.065	18
$Ni_{0.7}Co_{0.3}(OH)_2$	1541	2-800	3.42	19
Amorphous Co-Ni hydroxide	1911.5	0.25-5000	0.12	20
NiFe-LDH/NF	3680.2	4-800	0.59	21
CoFe LDH/PBA/NF	**5499**	**1-500**	**0.1**	**This work**
	2659	500-920		
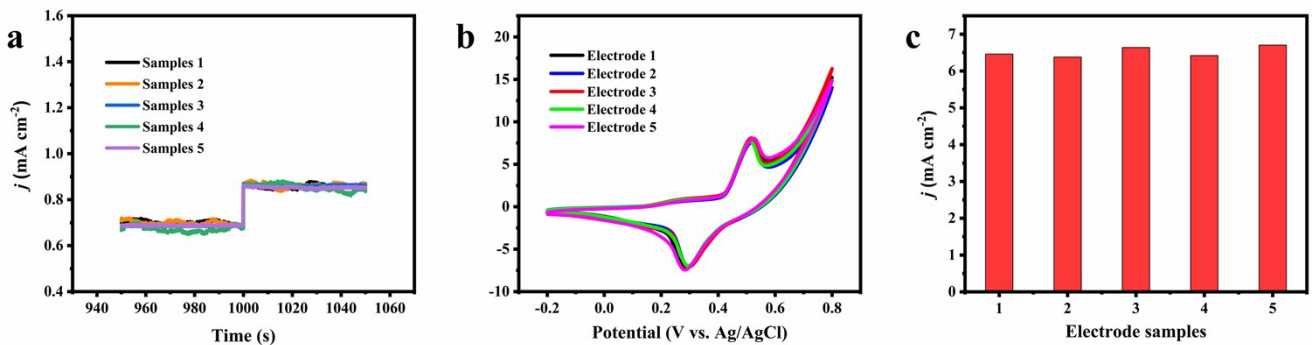
Fig. S8 (a) Amperometric responses obtained by five identical CoFeLDH/PBA/NF electrodes to 30 μM glucose in 0.1 M NaOH. (b) CV curves of five identical CoFeLDH/PBA/NF electrodes in 0.1 M NaOH at 50 mV s⁻¹. (c) The plot of oxidation peak current density and five CoFeLDH/PBA/NF electrodes.

The reproducibility of the CoFeLDH/PBA/NF electrode was evaluated based on two methods of amperometric response (Fig. S8a) and CV responses (Fig. S8b) according to reported literature. [12, 14] For

CV responses, five CoFeLDH/PBA/NF electrodes were fabricated in same condition. Their CV responses were measured in 0.1 M NaOH without glucose as shown in Fig. S8b, and corresponding relationship between oxide peak current density and five parallel electrodes was shown in Fig. S8c. The relative standard deviation (RSD) of only 2.81 % can be obtained, confirming their excellent reproducibility.
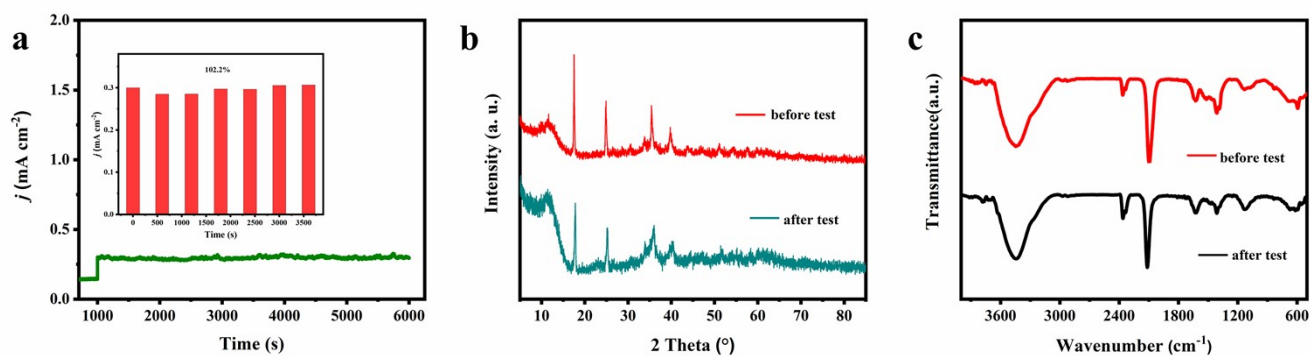

Fig. S9 (a) Amperometric response of CoFeLDH/PBA/NF electrode in 0.1 M NaOH solution with addition of 30 µM glucose at 0.5 V. (b) The XRD patterns, (c) FT-IR spectra of CoFeLDH/PBA/NF electrode after stability test.
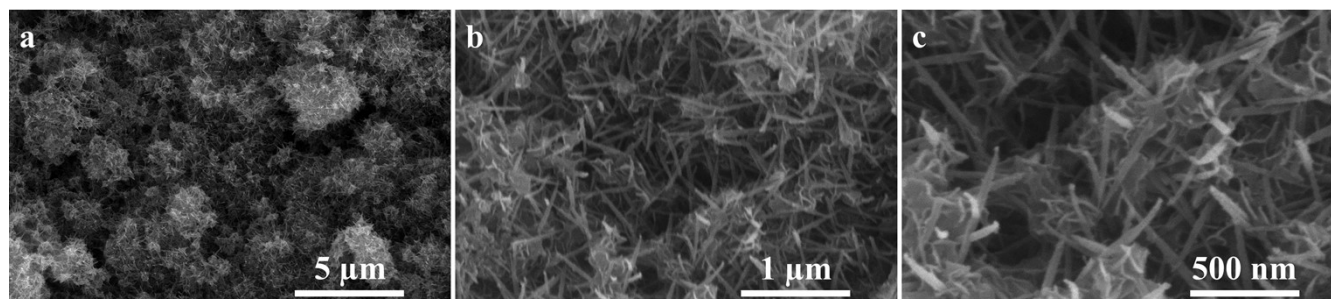

Fig. S10 (a-c) SEM images of CoFePBA/NF after stability test.

References

1 D. Xiong, C. Lu, C. Chen, J. Wang, J. Chen, F.-Y. Yi and X. Ma, *Mater. Chem. Front.*, 2021, **5**, 1388-1397.

2 C. Chen, D. Xiong, M. Gu, C. Lu, F. Y. Yi and X. Ma, *ACS Appl. Mater. Interfaces.*, 2020, **12**, 35365-35374.

3 J. Cui, Z. Li, K. Liu, J. Li and M. Shao, *Nanoscale Adv.*, 2019, **1**, 948-952.

4 L. Yu, H. Zhou, J. Sun, F. Qin, D. Luo, L. Xie and Z. Ren, *Nano. Energy.*, 2017, **41**, 327-336.

5 L. Wang, N. Wang, J. Wen, Y. Jia, S. Pan, H. Xiong, Y. Tang, J. Wang, X. Yang, Y. Sun, Y. Chen and P. Wan, *Chem. Eng. J.*, 2020, **397**, 125450.

6 F. Zhu, W. Liu, Y. Liu and W. Shi, *Chem. Eng. J.*, 2020, **383**, 123150.

7 D. Song, L. Wang, Y. Qu, B. Wang, Y. Li, X. Miao, Y. Yang and C. Duan, *J. Electrochem. Soc.*, 2019, **166**, B1681-B1688.

8 L. Wang, X. Miao, Y. Qu, C. Duan, B. Wang, Q. Yu and Z. Yin, *J. Electroanal. Chem.*, 2020, **858**, 113810.

9 S. Liu, W. Zeng, Q. Guo and Y. Li, *J. Mater. Sci.: Mater. Electron.*, 2020, **31**, 16111–16136.

10 D. Hwang, S. Lee, M. Seo and T. Chung, *Anal. Chim. Acta.*, 2018, **1033**, 1-34.

11 M. Wei, Y. Qiao, H. Zhao, J. Liang, T. Li, Y. Luo, S. Lu, X. Shi, W. Lu and X. Sun, *Chem. Commun.*, 2020, **56**, 14553-14569.

12 Q. Niu, W. Lu, C. Bao, M. Wei, Z. Chen and J. Jia, *J. Electroanal. Chem.*, 2020, **874**, 114507.

13 Y. Li, M. Xie, X. Zhang, Q. Liu, D. Lin, C. Xu, F. Xie and X. Sun, *Sens. Actuators B.*, 2019, **278**, 126-132.

14 R. Ahmad, M. Khan, P. Mishra, N. Jahan and A. Khosla, *J. Electrochem. Soc.*, 2021, **168**, 017501.

15 Z. Zhao, J. Ding, H. Zhou, R. Zhu and H. Pang, *CrystEngComm.*, 2019, **21**, 5455-5460.

16 J. Cui, Z. Li, K. Liu, J. Li and M. Shao, *Nanoscale Adv.*, 2019, **1**, 948-952.

17 M. Shao, X. Xu, J. Han, J. Zhao, W. Shi, X. Kong, M. Wei, D. G. Evans and X. Duan, *Langmuir.*, 2011, **27**, 8233-8240.

18 S. An, N. Shang, B. Chen, Y. Kang, M. Su, C. Wang and Y. Zhang, *J. Colloid. Interface. Sci.*, 2021, **592**, 205-214.

19 F. Sun, S. Wang, Y. Wang, J. Zhang, X. Yu, Y Zhou and J. Zhang, *Sensors.*, 2019, **19**, 2938.

20 H. Li, L. Zhang, Y. Mao, C. Wen and P. Zhao, *Nanoscale Res. Lett.,* 2019, **14**, 135.

21 Y. Lu, B. Jiang, L. Fang, S. Fan, F. Wu, B. Hu and F. Meng, *Electroanalysis.* 2017, **29**, 1755-1761.